

Studies of New 2,7-Carbazole (CB) Based Donor-Acceptor-Donor (D-A-D) Monomers as Possible Electron Donors in Polymer Solar Cells by DFT and TD-DFT Methods

Numbury Surendra Babu*^[a]

The new donor-acceptor-donor (D-A-D) monomers have been studied using density functional theory (DFT) and time-dependent density functional theory (TD-DFT) methods to evaluate the optoelectronic and electronic properties for bulk heterojunction (BHJ) organic solar cells. The TD-DFT method is combined with a hybrid exchange-correlation functional using the B3LYP method in conjunction with a polarizable continuum model (PCM) and a 6-311G basis set to predict the excitation energies and absorption spectra of all monomers. The predicted bandgap (E_g) of the monomers decreasing in the following

order $D1 < D2 < D3 < D4 < D5 < D6 < D7 < D9 < D8$. Furthermore, open-circuit voltage (V_{oc}) estimates for monomers with [6,6]-phenyl-C₇₁-butyric acid methyl ester (PC71BM) acceptor. The V_{oc} of the studied monomers ranges from 0.976 to 1.398 eV in the gas and from 1.109 to 1.470 eV in the solvent phase with PC71BM acceptor, which is sufficient for efficient electron injection into the acceptor's LUMO. The results show that theoretically, a maximum energy conversion efficiency of roughly 5% for D8 and 5.8% for D7.

Introduction


All the world's energy demands can be provided by solar cells. With new materials like semiconducting conjugated polymers in bulk heterojunction (BHJ)^[1-3] solar systems, manufacturing costs could be drastically lowered. Organic solar cells (OSCs) based on bulk heterojunction (BHJ) technology combine donor polymers with acceptor fullerene derivatives. Despite their many advantages over silicon solar cells (cheap cost, light-weight, ease of manufacture, transparency & flexibility), these cells have received substantial attention from the physical, chemical, and scientific areas.^[4,5] However, their broad bandgaps have hindered 3-hexylthiophene (P3HT) and poly[2-methoxy-5-(3',7'-dimethyloctyloxy)-p phenylenevinylene] (MDMOPPV's) capabilities (E_g). Thus recent investigations have looked into polymer architectures as a viable rival.^[6,7] Internal molecular charge transfer (ICT) from an electron-rich unit to an electron-deficient moiety has been frequently employed for conjugated polymers for many years.^[8-10] For the first time in history, new polymers can capture solar spectrum based on internal charge transfer (ICT). Low-performance solar cells have been made by Krebs^[11,12] and Reynolds.^[13,14] The power conversion efficiency (PCE) of polyfluorene derivatives ranges from 2.0 to 4.2%.^[15,16]

However, the low carrier mobility of these polymers has an adverse effect on device performance. Furthermore, the PCE values of benzothiadiazole and cyclopentadithiophene copolymers were quite interesting.^[17,18] As a result, it is possible to manufacture ICT polymers with low bandgap (E_g) and high carrier mobility.^[19]

Additionally, poly(2,7-carbazole) molecules can be used in BHJ solar cells. Poly(2,7-carbazole)s and poly(2,7-fluorene)s can be easily modulated in terms of their physical properties.^[20,21] Carbazole units, which are electron-rich compounds, can be used to make ICT polymers.^[22-24] It is also worth noting that poly(9-vinylcarbazole) (PVK) is one of the most extensively utilized photoconductive polymers nowadays. Polycarbazole materials with low solar cell efficiency were developed by K. Mullen in a preliminary study (0.6–0.8%).^[25] These polymers were poorly soluble and had little order. In recent studies, researchers have discovered a new polycarbazole derivative (PCDTBT),^[26] containing a secondary alkyl chain on the carbazole unit's nitrogen atom that has a good PCE (3.6%). It is possible to improve the electrical characteristics of polymeric materials.

The efficiency of BHJ solar cells can be estimated using various models.^[27] When it comes to air stability, the first thing a polymer needs is a low HOMO energy level (approximately –5.27% of SCE or 0.57 V).^[28] It also assures that the completed gadget has a high open circuit potential (V_{oc}). A polymer's LUMO energy level must be at least 0.2–0.3 eV more elevated than the acceptor's – [6,6]-phenyl-C₆₁-butyric acid methyl ester (PCBM).^[29,30] LUMO energy level is necessary for efficient electron transfer between the polymer and acceptor. A donor LUMO energy level of approximately 3.75–4.0 eV is considered ideal. A bandgap of between 1.2 and 1.9 eV is desirable, taking into account the solar spectrum and the open circuit potential of the solar cell. As a result, –5.2 to –5.8 eV should be the ideal range for polymer HOMO energy. It must also reduce the LUMO

[a] Prof. N. S. Babu
Computational Quantum Chemistry Lab
Department of Chemistry
College of Natural and Mathematical Sciences
The University of Dodoma
Donoma (Tanzania)
E-mail: nsbabusk@gmail.com

 © 2022 The Authors. Published by Wiley-VCH GmbH. This is an open access article under the terms of the Creative Commons Attribution Non-Commercial License, which permits use, distribution and reproduction in any medium, provided the original work is properly cited and is not used for commercial purposes.

energy level of PCDTBT (−3.60 eV) while retaining the HOMO energy level to increase a polymeric cell's performance (i.e., −5.45 eV).

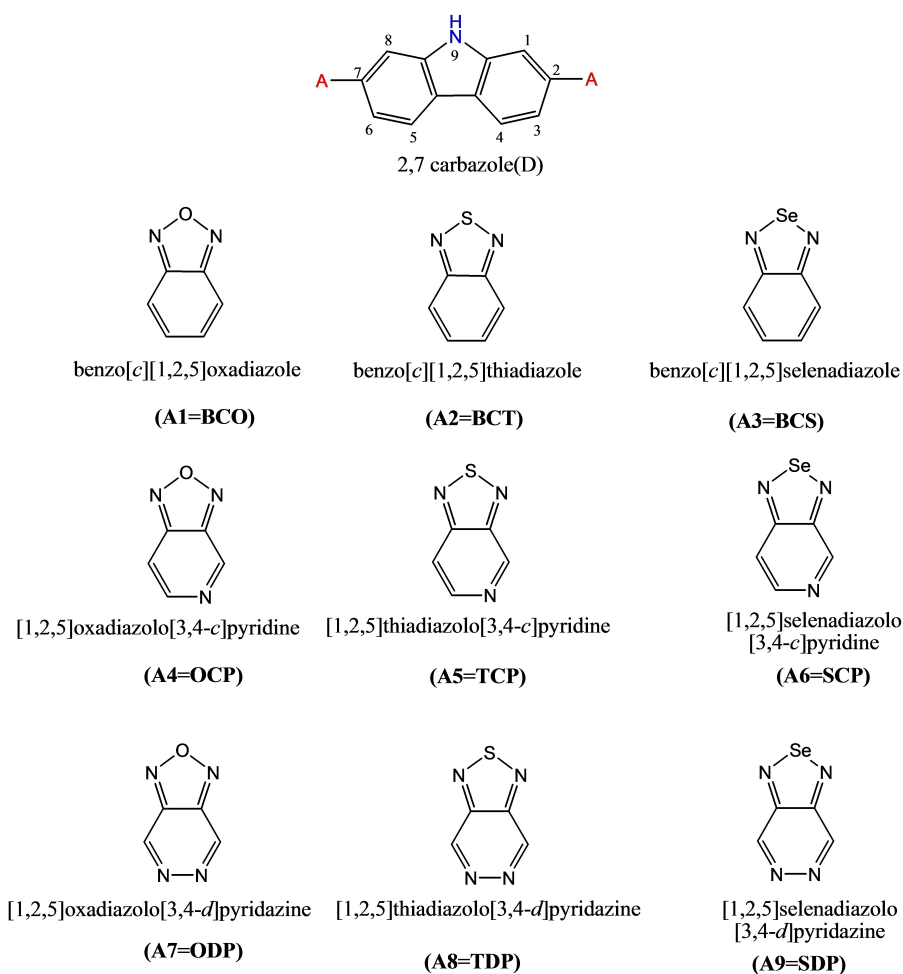
We used these data and theoretical models for solar cell devices to explore alternating polymeric architectures to discover the optimum poly(2,7-carbazole) derivatives.^[31,32] The HOMO and LUMO energy levels were calculated using quantum mechanics to evaluate their performance. Small organic molecule PCE improvements were made possible by the success of donor-acceptor copolymers, in which electron-rich and electron-deficient moieties were attached to one other. These structural frameworks have been constructed as well as oligomers and oligomer patterns.^[33]

It is possible to modify the characteristics of these polymers as organic semiconductors by changing the donor and acceptor units. D-A-D is a critical component for charge separation and molecular architecture governing charge transfer. Its bandgap (E_g) is lowered, its charge change is significant, and its visible light absorption is enhanced due to the high overlap of D and A molecular orbitals. Therefore, one of the criteria for developing a high photocurrent was synthesizing donor and acceptor materials with complementary absorption properties. The

study's uniqueness is generated from these preliminary findings and theoretical models by using innovative donor-acceptor donor monomers as a 2,7-carbazole donor and benzothiazole derivatives as acceptors.

Computational Calculation Details

Carbazoles, 2,7-carbazoles, were employed in this work as donors (D) and acceptors (A1–A9) (Scheme 1). We have created small-molecule organic photovoltaic (OPV) donors of the D-A-D type. There are many D and A unit combinations that it would be impossible to develop small molecule OPV donors without first running them via pre-synthesis simulated screenings. We have clearly defined molecular orbital (MO) energy levels, bandgap (E_g), UV/Vis absorption spectra, and PCEs of different D-A-D polymer donors using density functional theory (DFT) and time-dependent DFT (TD-DFT) calculations at the B3LYP/6-311G level.^[34–38] The 6-311G basis set was used for all computations. The Gaussian 09 package^[39] was used to calculate the density (DFT) and time-dependent (TD-DFT) functional^[40] in gas and chlorobenzene solvents. TD-DFT/B3LYP



Scheme 1 Donor-Acceptor- Donor (D-A-D) monomers in the present study.

Scheme 1. Donor-Acceptor-Donor (D-A-D) monomers in the present study.

method was employed to predict the vertical excitation energy and electronic absorption spectra of studied monomers. This approach, which has been around for more than two decades, is one of the most effective ways to deal with bulk solvent effects in ground and excited states. This work used the *Polarizable Continuum Model* (PCM)^[41] model to compute the excitation energy. Using TD-DFT computations for DFT optimized geometries, oscillator strengths and excited-state energy were studied. The total density states (TDOS) were visualized using the GaussSum program.^[42]

Results and Discussion

Electronic Properties

DFT/B3LYP and a 6-311G basis set have been used to optimize all of the studied donors (D-A-D) monomers, and the optimized geometries are shown in Figure 1. It's vital to note that theoretical components are essential in investigating organic solar cells, which we use as an example of their electrical applications. To determine whether or not photovoltaic devices work, the HOMO and LUMO energy levels of the donor and

acceptor components must be considered. As illustrated in the experiment, an empirical formula may be used to determine HOMO and LUMO energies by changing voltage as they occur in an electrochemical cycle. For the HOMO and LUMOS, however, DFT is theoretically possible. Furthermore, when calculating HOMO and LUMO energy levels in a thin film, DFT does not consider the effects of solid-state packing, which can impact the energy levels of molecules. Therefore, it is possible to gather information about similar oligomers or polymers by comparing the anticipated energy levels, even if they are inaccurate.

For frontier molecular orbitals (FMO), orbitals for the nine monomers are shown in the solvent phases in Figure 2. The FMO distribution of all nine monomers is nearly identical. While all HOMOs exhibit typical aromatic features with electron delocalization over the entire conjugated molecule, they are concentrated at the donor parts and conjugated spacers, whereas LUMOs focus on the acceptor moieties (A). Anti-bonding properties exist in the HOMO between successive subunits. While all oligomers have a bonding character between the two adjacent pieces, the LUMO of all oligomers corresponds to the π^* electronic transition in the lowest-lying singlet states. Photo excited electrons can be more

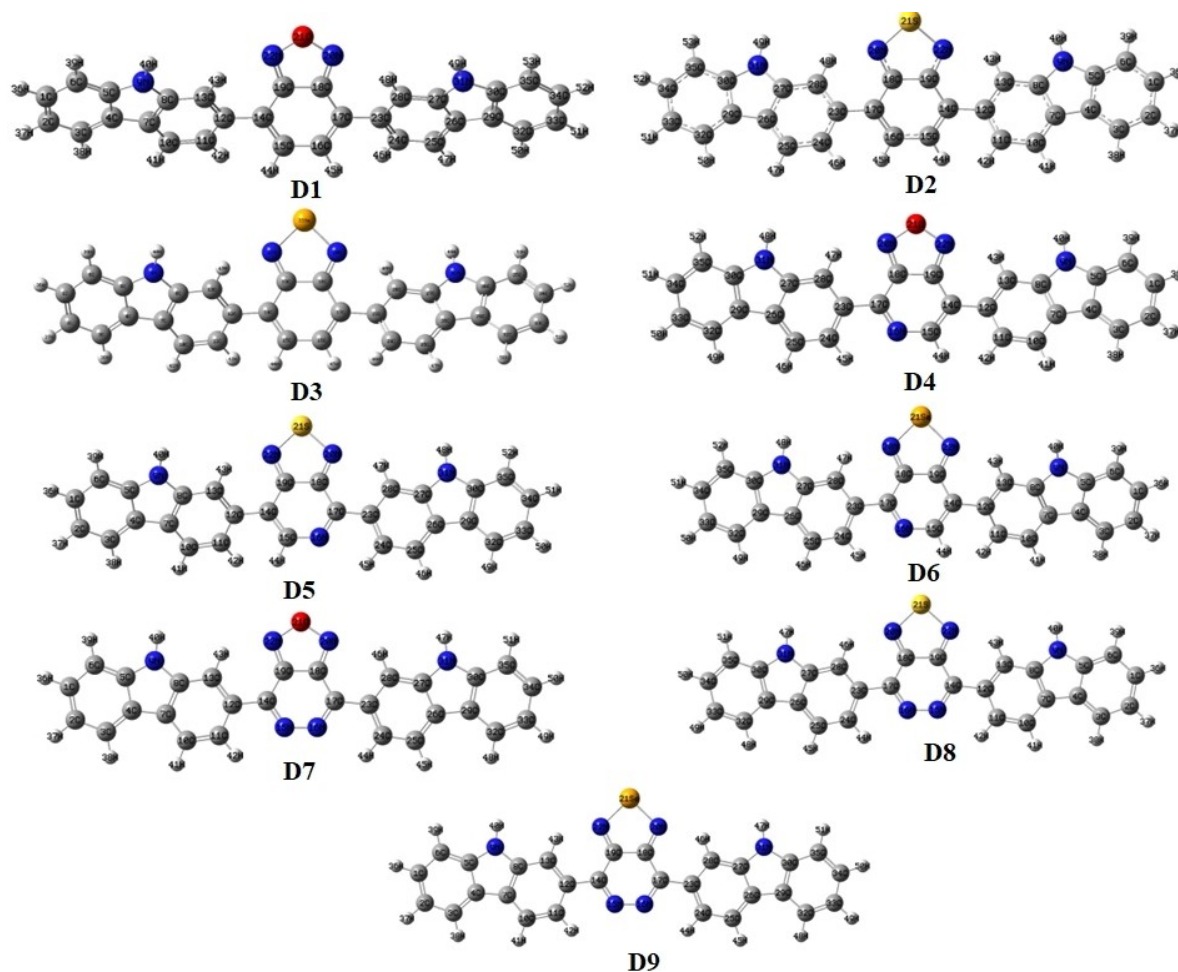


Figure 1. Optimized geometries of the studied molecules obtained by B3LYP/6-311G in the gas phase.

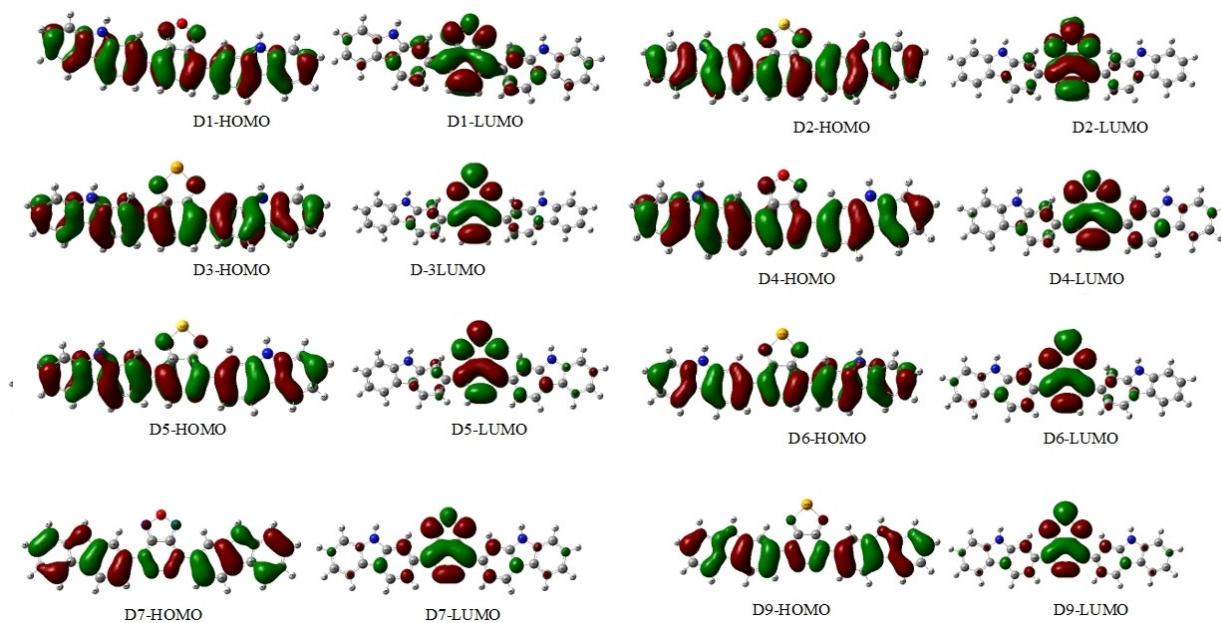


Figure 2. Representation of the frontier molecular orbitals (HOMO and LUMO) obtained from DFT//B3LYP/6-311G calculations in the solvent phase.

easily injected into a semiconductor's LUMO if transferred from a donor moiety into an acceptor moiety during excitation (PC71BM). All compounds contribute significantly to LUMOs, resulting in solid electronic coupling with PC71BM surface upon photo excitation electrons, thus improving electron injection efficiency and, as a result, increasing the short-circuit current density (J_{sc}) by increasing the short-circuit current density.

For nine monomers (D1–D9), B3LYP/6-31G predicted the HOMO, LUMO, and band gaps using the B3LYP/6-311G level in Table 1. For D1, these are the HOMO/LUMO energies: $-5.3726/-2.4354$ eV; for D2, these are $-5.3527/-2.7491$ eV; for D3, these are $-5.2765/-2.6762$ eV; and for D4, these are $-5.5570/-3.1491$ eV. For D9, the energy gap is $-5.4996/-3.4038$ eV, with equivalent energy gaps of 2.9372 eV for D1, 2.6036 eV for D2, 2.6003 eV for D3, 2.4079 eV for D4, 2.2980 eV for D5, 2.2934 eV for D6, 2.2096 eV for D7, and 2.096 eV for D8.

Table 1 shows the HOMO-LUMO energy gaps (E_g) for studied D-A-D monomers. Every donor has a lower bandgap (E_g) value except for the D8 and D9 monomers. In both gas and solvent phases, the predicted bandgap (E_g) of the monomers decreasing in the following order $D1 < D2 < D3 < D4 < D5 < D6 < D7 < D9 < D8$. Intramolecular charge transfer strongly influences the absorption spectra of D8 and D9, which is linked to the impact of the electron-donor unit, which is particularly potent in these two monomers. This means that the acceptor unit's inductive effects considerably impact the band gaps of the molecules formed. Figure 3 shows the FMO energy levels and energy gaps of the all monomers model. HOMO energy levels of the D1–D9 monomers in the gas and solvent phases are shown in Table 1, indicating that these systems may be stable in the air with BHJSC and PC71BM.

In addition, their results showed that sulfur, nitrogen, and oxygen groups could help close energy gaps. SCP acceptor unit's more substantial electron-donor capabilities should be

Table 1. Calculated E_{HOMO} , E_{LUMO} energy levels, bandgap (E_g) values of the studied monomers obtained by DFT/B3LYP/6-311G level.

S.No	monomer (D)	gas HOMO [eV]	LUMO [eV]	chlorobenzene HOMO [eV]	LUMO [eV]	gas E_g [eV]	solvent E_g [eV]
1	D1	-5.37	-2.43	-5.46	-2.54	2.93	2.91
2	D2	-5.35	-2.74	-5.46	-2.83	2.60	2.63
3	D3	-5.27	-2.67	-5.40	-2.73	2.60	2.67
4	D4	-5.55	-3.14	-5.64	-3.28	2.40	2.36
5	D5	-5.44	-3.14	-5.55	-3.21	2.29	2.34
6	D6	-5.36	-3.07	-5.49	-3.11	2.29	2.38
7	D7	-5.69	-3.48	-5.77	-3.60	2.21	2.16
8	D8	-5.56	-3.48	-5.67	-3.52	2.07	2.15
9	D9	-5.50	-3.40	-5.63	-3.42	2.09	2.21
10	PC ₇₁ BM	-6.10	-4.30	-	-	-	-
11	PC ₆₀ BM	-5.98	-3.22	-	-	-	-

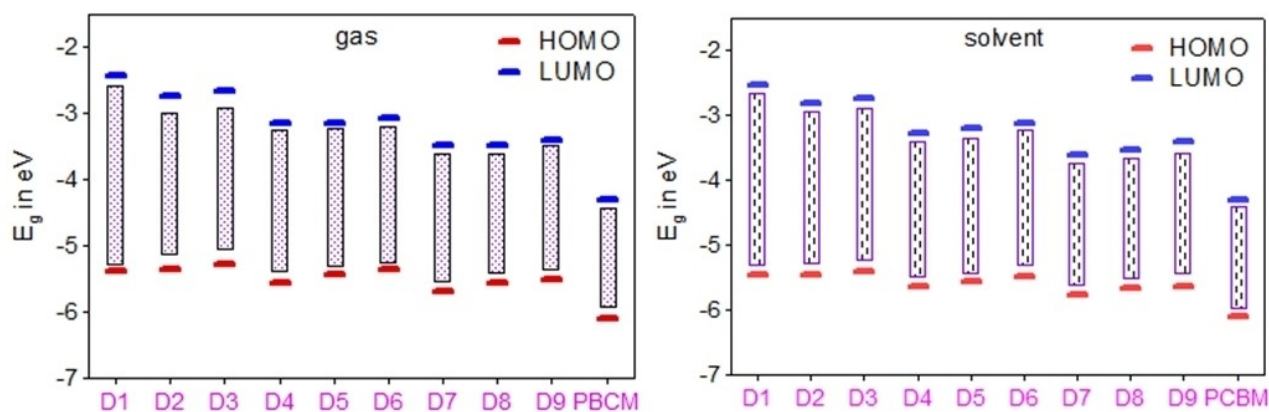


Figure 3. The HOMO and LUMO energy levels of the studied D-A-D monomers at DFT/B3LYP level with a 6-311G basis set.

directly linked to the more significant energy gap between D8 and D9 monomers in that case. According to these findings, acceptor units appear to have a significant impact on LUMO distribution and, as a result, HOMO-LUMO energy gaps. D8 and D9, which are the most planar and so conjugated, may be responsible for the disparity in the distribution of the LUMO orbital among the built systems.

Photovoltaic Properties

There are several essential parameters, including the short-circuit current density (J_{SC}), the open-circuit voltage (V_{OC}), the fill factor (FF), and the incident photon-to-current efficiency that can be used to compare and quantify solar cell performance (P_{inc}). Therefore, Equation (1) was used to calculate the power conversion efficiency (PCE).

$$PCE = \frac{V_{OC} J_{SC} FF}{1000 W / m^2} \quad (1)$$

A device's form and charge carriers' lifetime and mobility affect the flow of this fluid when no voltage is provided.^[43]

Assuming the photo charge loss is taken into account, one may calculate the maximal open-circuit voltage (V_{OC}) by subtracting the donor's HOMO (conjugated molecule) from the acceptor's LUMO (conjugated molecule). The V_{OC} was found to have a low dependence on the electrodes' work functions. Therefore, the open-circuit voltage V_{OC} of the BHJ solar cell was calculated using the following formula:^[44,45]

$$V_{OC} = \frac{1}{e} \left(|E_{HOMO}^{Donor}| - |E_{LUMO}^{PCBM}| \right) - 0.3 \quad (2)$$

This equation has two components: the elementary charge and the empirical component. For the PC71BM, Scharber et al.^[45] used Equation (2), using the PC71BM LUMO energy of 4.3 eV. Another reason for high solar cell efficiency is due to the low LUMO of conjugated molecules and high LUMO of the electron acceptor (PC71BM), which raises the value of V_{OC} .^[46,47]

To provide efficient electron injection into the acceptor's LUMO, the predicted open-circuit voltage V_{OC} of the examined molecules ranges from 0.976 eV in the gas and from 1.109 to 1.470 eV for PC71BM. While this discrepancy is more than 0 eV, Table 2 demonstrates that the differences in LUMO energy levels between the newly produced donors (D1–D9) and the acceptor of PC71BM are more significant than this value

Table 2. The open-circuit voltage V_{OC} (eV), $LUMO_{donor} - LUMO_{acceptor}$ ($L_D - L_A$) and first singlet excitation energy (E_{OPT}), the exciton binding energy (E_B) of the studied monomers.

Monomer	V_{OC} [eV]/ PC ₇₁ BM −4.3		$L_D - L_A$ (PC71BM)		E_{OPT}		E_B	
	Gas	Chloro- benzene	gas	chloro-benzene	gas	chloro-benzene	gas	chloro-benzene
D1	1.07	1.17	1.87	1.75	2.56	2.47	0.38	0.45
D2	1.05	1.17	1.55	1.47	2.17	2.16	0.43	0.48
D3	0.98	1.11	1.62	1.56	2.17	2.17	0.43	0.50
D4	1.26	1.34	1.15	1.02	2.06	1.95	0.35	0.41
D5	1.14	1.26	1.16	1.09	1.92	1.91	0.38	0.43
D6	1.06	1.20	1.23	1.19	1.91	1.95	0.38	0.44
D7	1.40	1.47	0.81	0.70	1.82	1.73	0.39	0.44
D8	1.26	1.38	0.81	0.77	1.69	1.73	0.38	0.43
D9	1.20	1.34	0.90	0.88	1.72	1.80	0.38	0.42

(LUMO_D–LUMO_A), ensuring that electrons from the donor to the acceptor are effectively transferred (PC71BM). This results in the transport of electrons from donor monomers to PC71BM's LUMO. As a result, all of the molecules examined can be used as BHJ in an organic sensitized solar cell because of the electron injection process from the excited molecule to the conduction

band of PC71BM and subsequent regeneration. Consequently, the optimum donor may be evaluated based on the [E_{LUMO} (donor)–E_{LUMO} (acceptor)] energy and bandgap location of the donor (Figure 4). D8 and D7 polymer solar cells (PSCs) theoretically have a maximum energy conversion efficiency of about 5% and 5.8%, respectively.^[48,49]

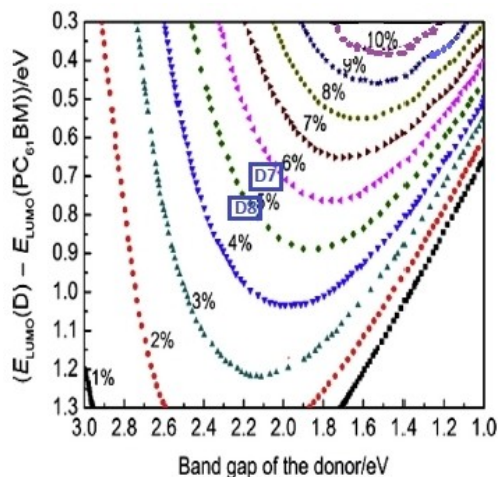


Figure 4. Scharber diagrams to estimate PCEs (%) for the copolymers D7 and D8.

Optical Properties

The TD-DFT/B3LYP/6-31G level was used to calculate electronic properties and absorption spectra in the gas and chlorobenzene solvent phases. The calculated absorption wavelengths (λ_{\max}), oscillator strengths (f) and vertical excitation energies (E) for gaseous phase and solvent (chloroform) were carried out and listed in Tables 3 and 4 in the gas and solvent phase respectively. ICT transitions were present in the spectra of all compounds, with a prominent concentrated band at higher energies spanning from 484.20 to 721.72 nm for the gas phase and 502.39 to 690.34 nm for chloroform solvent. Excitation energy changes in decreasing order as donor group changes in Tables 3 and 4 of this paper. There is a redshift in the solvent phase between the D9 > D8 > D7 > D6 > D5 > D4 > D3 > D2 > D1 sequence and the D8 > D7 > D9 > D6 > D5 > D4 > D3 > D2 > D1 sequence. In gas-phase and chloroform solution, the

Table 3. Computed maximum absorption wavelength (λ_{\max}), excitation energies (Ex), oscillator strengths (f_{os}), major molecular orbital assignments and configuration interaction (C.I) of designed D-A-D monomers in the gas phase at the TD-DFT/B3LYP/6-311 G level of theory.

Monomer	Transition state	λ_{\max} [nm]	Ex	f_{os}	Major MO Assignments	C.I
D1	S ₀ →S ₁	484.20	2.56	0.76	HOMO→LUMO	98.87
	S ₀ →S ₂	456.23	2.72	0.00	HOMO-1→LUMO	98.80
	S ₀ →S ₃	455.93	2.72	0.01	HOMO-2→LUMO	99.02
D2	S ₀ →S ₁	571.56	2.17	0.35	HOMO→LUMO	98.66
	S ₀ →S ₂	527.44	2.35	0.01	HOMO-1→LUMO	98.90
	S ₀ →S ₃	526.94	2.35	0.00	HOMO-2→LUMO	99.27
D3	S ₀ →S ₁	572.06	2.17	0.35	HOMO→LUMO	98.91
	S ₀ →S ₂	523.56	2.37	0.00	HOMO-1→LUMO	99.16
	S ₀ →S ₃	521.34	2.38	0.00	HOMO-2→LUMO	99.15
D4	S ₀ →S ₁	601.77	2.06	0.46	HOMO-1→LUMO	13.55
					HOMO→LUMO	84.77
	S ₀ →S ₂	596.90	2.08	0.13	HOMO-1→LUMO	85.76
					HOMO-2→LUMO	13.12
D5	S ₀ →S ₃	580.85	2.13	0.01	HOMO-3→LUMO	97.16
	S ₀ →S ₁	646.95	1.92	0.40	HOMO→LUMO	98.22
	S ₀ →S ₂	631.56	1.96	0.02	HOMO-1→LUMO	98.90
D6	S ₀ →S ₃	608.74	2.04	0.01	HOMO-2→LUMO	98.81
	S ₀ →S ₁	648.26	1.91	0.41	HOM→LUMO	98.87
	S ₀ →S ₂	625.38	1.98	0.01	HOMO-1→LUMO	99.35
D7	S ₀ →S ₃	602.12	2.06	0.00	HOMO-2→LUMO	99.01
	S ₀ →S ₁	683.05	1.82	0.02	HOMO-2→LUMO	70.93
					HOMO→LUMO	28.24
	S ₀ →S ₂	682.52	1.82	0.00	HOMO-1→LUMO	99.12
	S ₀ →S ₃	654.25	1.90	0.60	HOMO-2→LUMO	28.23
					HOMO-1→LUMO	71.43
D8	S ₀ →S ₁	732.95	1.69	0.67	HOMO-2→LUMO	53.61
					HOMO→LUMO	45.97
	S ₀ →S ₂	730.23	1.70	0.00	HOMO-1→LUMO	99.44
	S ₀ →S ₃	712.68	1.74	0.40	HOMO-2→LUMO	45.77
D9	S ₀ →S ₁	721.73	1.72	0.13	HOMO→LUMO	53.76
					HOMO-1→LUMO	40.27
					HOMO→LUMO	59.35
	S ₀ →S ₂	717.51	1.73	0.00	HOMO-1→LUMO	99.44
	S ₀ →S ₃	705.87	1.76	0.32	HOMO-2→LUMO	59.10
					HOMO→LUMO	40.34

Table 4. Computed maximum absorption wavelength (λ_{\max}), excitation energies (Ex), oscillator strengths (f_{os}), major molecular orbital assignments and configuration interaction (C.I) of designed D-A-D monomers in chlorobenzene solvent at the TD-DFT/B3LYP/6-311 G level of theory.

Monomer	Transition state	λ_{\max} [nm]	Ex	f_{os}	Major MO Assignments	C.I
D1	$S_0 \rightarrow S_1$	502.39	2.47	0.82	HOMO \rightarrow LUMO	98.87
	$S_0 \rightarrow S_2$	469.32	2.64	0.01	HOMO-1 \rightarrow LUMO	98.80
	$S_0 \rightarrow S_3$	469.04	2.64	0.01	HOMO-2 \rightarrow LUMO	99.02
D2	$S_0 \rightarrow S_1$	574.55	2.16	0.40	HOMO \rightarrow LUMO	99.35
	$S_0 \rightarrow S_2$	529.53	2.34	0.01	HOMO-1 \rightarrow LUMO	99.08
	$S_0 \rightarrow S_3$	529.24	2.34	0.00	HOMO-2 \rightarrow LUMO	99.13
D3	$S_0 \rightarrow S_1$	570.27	2.17	0.47	HOMO \rightarrow LUMO	99.19
	$S_0 \rightarrow S_2$	516.37	2.40	0.00	HOMO-1 \rightarrow LUMO	99.23
	$S_0 \rightarrow S_3$	513.80	2.41	0.00	HOMO-2 \rightarrow LUMO	99.30
D4	$S_0 \rightarrow S_1$	636.88	1.95	0.66	HOMO \rightarrow LUMO	99.37
	$S_0 \rightarrow S_2$	622.74	1.99	0.01	HOMO-2 \rightarrow LUMO	99.17
	$S_0 \rightarrow S_3$	616.30	2.01	0.02	HOMO-1 \rightarrow LUMO	99.30
D5	$S_0 \rightarrow S_1$	649.01	1.91	0.52	HOMO \rightarrow LUMO	98.38
	$S_0 \rightarrow S_2$	624.84	1.98	0.01	HOMO-2 \rightarrow LUMO	99.10
	$S_0 \rightarrow S_3$	614.62	2.02	0.07	HOMO-1 \rightarrow LUMO	99.11
D6	$S_0 \rightarrow S_1$	636.19	1.95	0.54	HOMO \rightarrow LUMO	96.92
	$S_0 \rightarrow S_2$	604.61	2.05	0.01	HOMO-1 \rightarrow LUMO	96.82
	$S_0 \rightarrow S_3$	593.61	2.09	0.01	HOMO-2 \rightarrow LUMO	2.31
D7	$S_0 \rightarrow S_1$	716.93	1.73	0.00	HOMO-1 \rightarrow LUMO	99.12
	$S_0 \rightarrow S_2$	716.76	1.73	0.01	HOMO-2 \rightarrow LUMO	98.88
	$S_0 \rightarrow S_3$	692.00	1.79	0.75	HOMO \rightarrow LUMO	98.87
D8	$S_0 \rightarrow S_1$	718.72	1.73	0.08	HOMO-2 \rightarrow LUMO	99.46
	$S_0 \rightarrow S_2$	717.43	1.73	0.00	HOMO \rightarrow LUMO	42.67
	$S_0 \rightarrow S_3$	705.23	1.76	0.55	HOMO-1 \rightarrow LUMO	56.83
D9	$S_0 \rightarrow S_1$	690.35	1.80	0.22	HOMO-2 \rightarrow LUMO	56.84
	$S_0 \rightarrow S_2$	687.48	1.80	0.00	HOMO \rightarrow LUMO	42.92
	$S_0 \rightarrow S_3$	681.58	1.82	0.40	HOMO-1 \rightarrow LUMO	37.11
					HOMO-2 \rightarrow LUMO	20.61
					HOMO \rightarrow LUMO	79.04

transition from HOMO to LUMO is the most likely transition from the ground state to an excited state, and this electronic absorption corresponds to the transition from the molecular orbital HOMO to the LUMO excited state and is a π^* transition.

Figures 5 and 6 show that all molecules in the visible region (abs > 700 nm) have only one band (Figure 5&6), suggesting that the solar cells linked with D7 and D8 may be able to harvest more light at longer wavelengths, benefiting the photo-

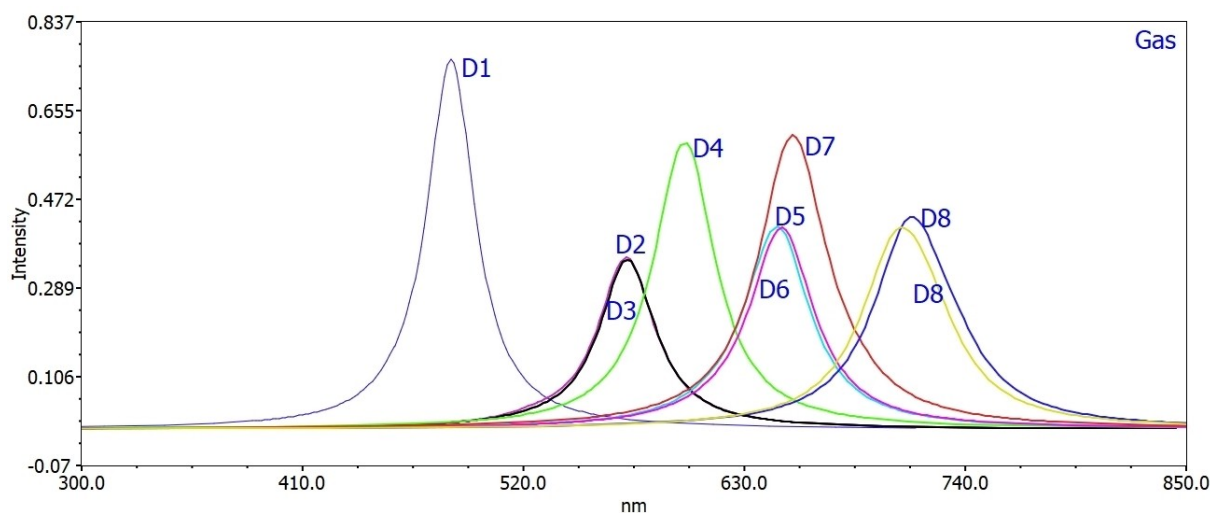


Figure 5. Simulated UV-Visible optical absorption spectra of the studied carbazole copolymer monomers (D-A-D) calculated by TD/DFT/B3LYP/6-311 G level in the gas phase.

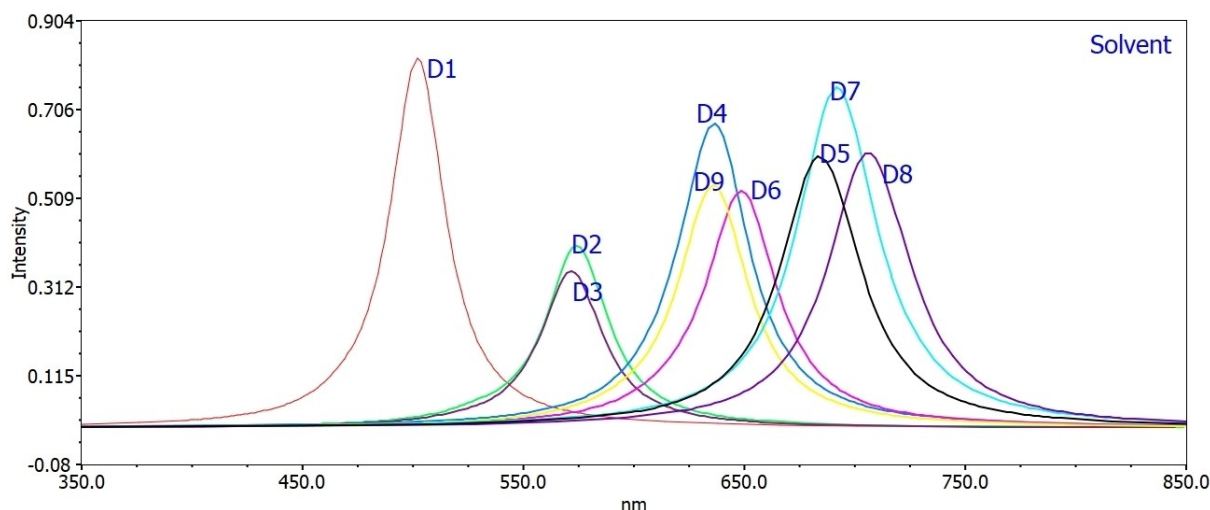


Figure 6. Simulated UV-Visible optical absorption spectra of the studied carbazole copolymer monomers (D-A-D) calculated by TD/DFT/B3LYP/6-311 G level in the solvent phase.

to-electric conversion efficiency. As a result, the acceptors can fine-tune the transition at the lowest point.

Quantum Chemical Parameters

Calculating chemical potential, electronegativity, and chemical hardness can be done using HOMO and LUMO energy values for monomers [Eq. (3-5)].^[50]

Chemical potential

$$\mu = \frac{(E_{HOMO} + E_{LUMO})}{2} \quad (3)$$

Chemical hardness

$$\eta = \frac{(E_{LUMO} - E_{HOMO})}{2} \quad (4)$$

Electronegativity

$$\chi = -\frac{(E_{HOMO} + E_{LUMO})}{2} \quad (5)$$

Electronic charge asymmetry is common in molecules that have a significant dipole moment. Due to the effect of an external electric field, they may be more sensitive to changes in their electronic structure and features. D8 and D9 monomers have a much higher dipole moment than the other monomers in Table 5, for example. In another way, we may say that some monomers are more reactive than others. Indeed, these monomers are more likely to liberate electrons from PCBM than other monomers.

In contrast to the nine monomers (D1, D2, D3, D4, D5, D6, D7, and D9), PCBM has the lowest chemical potential (=4.9) (see Table 5). This indicates that electrons are more likely to escape from compound Pi, which has a high chemical potential than PC71BM, a slight chemical possibility. Consequently, PC71BM is an electron acceptor, whereas the other monomers studied are electron donors. Furthermore, according to electronegativity, PC71BM has a higher value than any other monomer (D1 through 9) in terms of electronegativity (Table 5). As a result, electrons from other compounds can be attracted to the

Table 5. Calculated dipole moment (ρ) in Debye units and other quantum parameters chemical as electronegativity (χ), chemical potential (μ) and chemical hardness (η) values of the studied monomers obtained by B3LYP/6-311G level.

monomer	gas μ [eV]	η [eV]	χ [eV]	ρ	solvent μ [eV]	η [eV]	χ [eV]	ρ
D1	-3.904	1.469	3.904	1.724	-4.006	1.460	4.006	2.430
D2	-4.051	1.302	4.051	1.793	-4.150	1.319	4.150	2.447
D3	-3.976	1.300	3.976	1.532	-4.072	1.337	4.072	1.884
D4	-4.353	1.204	4.353	0.778	-4.462	1.180	4.462	1.175
D5	-4.291	1.149	4.291	2.659	-4.386	1.172	4.386	3.589
D6	-4.216	1.147	4.216	3.773	-4.306	1.192	4.306	5.143
D7	-4.594	1.105	4.594	2.516	-4.687	1.084	4.687	3.583
D8	-4.525	1.037	4.525	4.706	-4.603	1.075	4.603	6.601
D9	-4.452	1.048	4.452	5.845	-4.528	1.108	4.528	8.222
PCBM	-4.925	2.350	4.925	-	-	-	-	-

PC71BM molecule. We also see that the PCBM compound has a high chemical hardness (η) value compared to other monomer donors; this shows that the PC71BM is challenging to release electrons from, whereas the other compounds are good candidates for providing electrons for the PC71BM (see Table 5).

Density of States (DOS)

A great way to demonstrate the importance of molecular orbitals in chemical bonding is to use DOS charts. The DOS plot data may be an overlapping population of molecular orbitals. DOS also shows the orbital group composition part of the molecular orbital. DOS graphs in gas and solvent phases are depicted in Figures 7 and 8. In the energy range from 7.0 to 13 eV, the probability of localized states forming increases dramatically. The graph shows the orbital properties of various energy levels. Orbital of carbon and 'essential orbital functions' in the frontier molecular orbital contribute fundamentally. It is possible to employ organic solar cells based on V_{OC} values because electron injection into the acceptor's conduction band and subsequent regeneration are allowed in photovoltaic cells.

Conclusions

Density functional theory was used to study the properties of 2,7-carbazole donors and benzothiazole-based acceptors. Electrical and optical properties can be dramatically altered and improved by changing the chemical structure of pure materials. The following are some final thoughts: Band gaps in the solvent phase are expected to be in the range of 2.151–2.919 eV, according to DFT-B3LYP/6-31G calculations. The minuscule bandgap is due to increased electron displacement between the donor and acceptor spacers. Intramolecular charge transfer is significantly impacted by the lower E_g of D7 and D8 monomers than other monomers. For PC71BM, the open-circuit voltage V_{OC} ranges from 1.109 to 1.470 eV, suitable for efficient electron injection. All of the molecules studied can be used as BHJs since electron injection into the conduction band of PC71BM, and subsequent regeneration is possible in an organic sensitive solar cell. D7 can achieve a maximum power conversion efficiency of 5%, and D8 can reach a maximum power conversion efficiency of 3%. At least TD/B3LYP/6-31G TD-DFT calculations were used to predict the optical transitions; the starting vertical excitation energies (E) were varied in decreasing order for the gas phase: There is a redshift in the

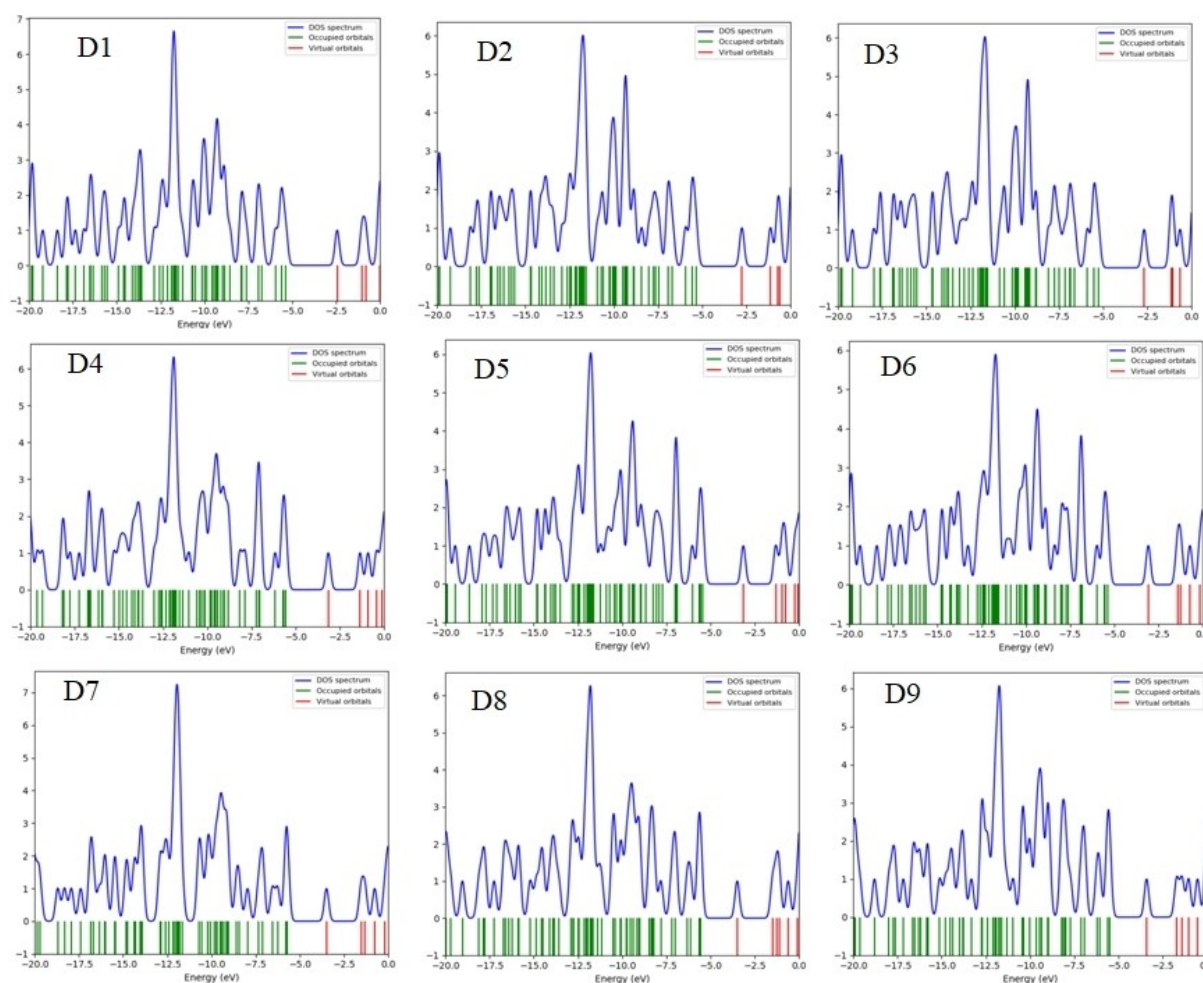


Figure 7. The density of states (DOS) plots for studied D-A-D monomers in gas

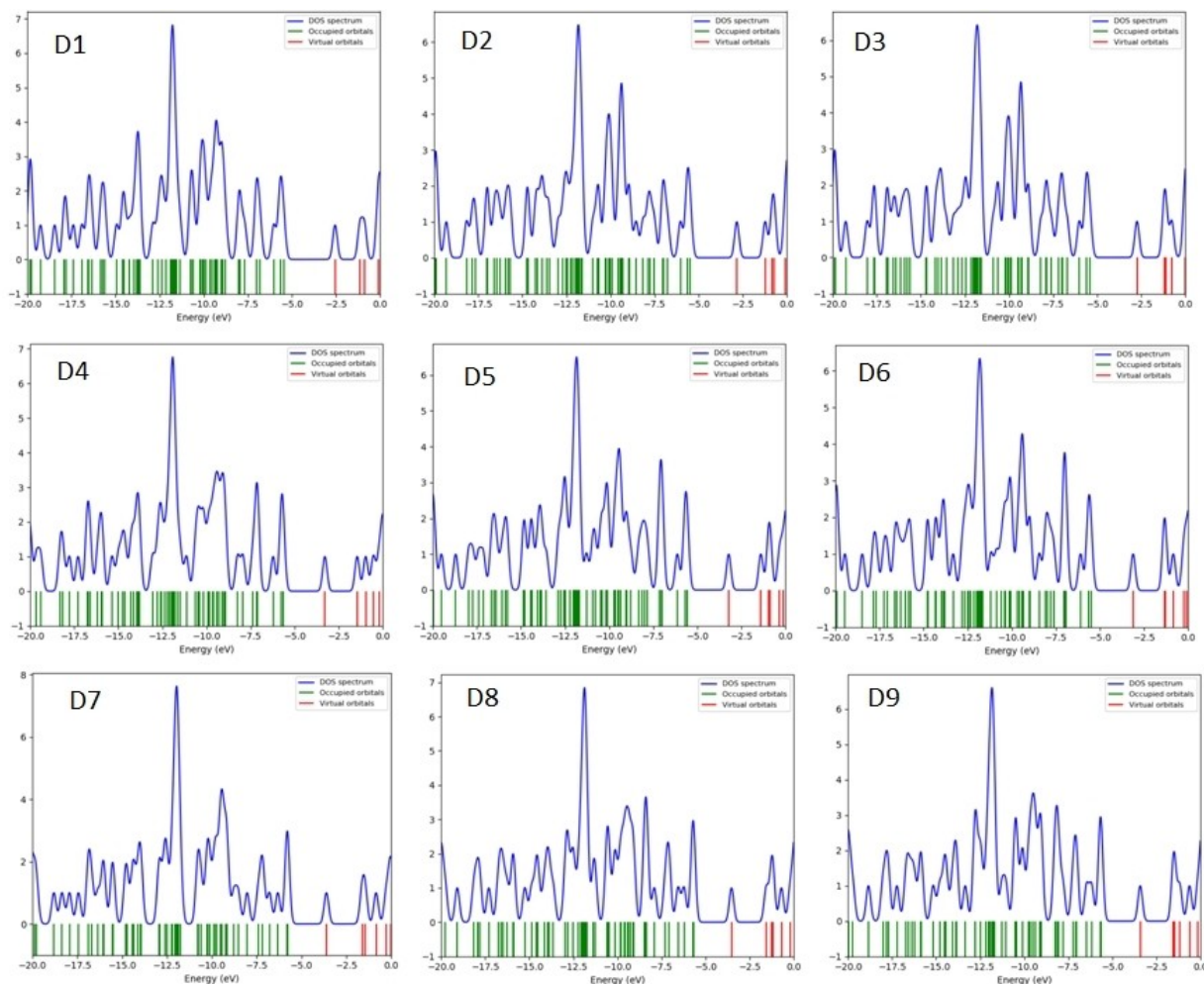


Figure 8. Density of states (DOS) plots for studied D-A-D monomers in the solvent chlorobenzene.

solvent phase between the $D9 > D8 > D7 > D6 > D5 > D4 > D3 > D2 > D1$ sequence and the $D8 > D7 > D9 > D6 > D5 > D4 > D3 > D2 > D1$ sequence. When it comes to solar cell photoelectric conversion efficiency, D7 and D8 may capture more light at longer wavelengths. As a result, the acceptors can fine-tune the transition at the lowest point.

Conflict of Interest

The authors declare no conflict of interest.

Data Availability Statement

The data that support the findings of this study are available on request from the corresponding author. The data are not publicly available due to privacy or ethical restrictions.

Keywords: 2,7-carbazole · D-A-D monomers · DFT/TD-DFT method · Optoelectronic properties · open-circuit voltage

- [1] K. M. Coakley, M. D. McGehee, *Chem. Mater.* **2004**, *16*, 4533–4542.
- [2] S. Günes, H. Neugebauer, N. S. Sariciftci, *Chem. Rev.* **2007**, *107*, 1324–1338.
- [3] M. Wang, D. Cai, Z. Yin, S. C. Chen, C. F. Du, Q. Zheng, *Adv. Mater.* **2016**, *28*, 3359–3365.
- [4] Y. Xia, J. Fang, P. Li, B. Zhang, H. Yao, J. Chen, J. Ding, J. Ouyang, A. C. S. *Appl. Mater. Interfaces* **2017**, *9*, 19001–19010.
- [5] E. A. A. Arbab, B. A. Taleatua, G. T. Mola, *Mater. Sci. Semicond. Process.* **2015**, *40*, 158–161.
- [6] J. Alstrup, K. Norrman, M. Jørgensen, F. C. Krebs, *Sol. Energy Mater. Sol. Cells.* **2006**, *90*, 2777–2792.
- [7] M. L. Chabiny, R. A. Street, J. E. Northrup, *Appl. Phys. Lett.* **2007**, *90*, 123508–3.
- [8] H. A. M. Van Mullekom, J. A. J. M. Vekemans, E. E. Havinga, E. W. Meijer, *Mater. Sci. Eng.* **2001**, *32*, 1–40.
- [9] A. Ajayaghosh, *Chem. Soc. Rev.* **2003**, *32*, 181–191.
- [10] J. Roncali, *Macromol. Rapid Commun.* **2007**, *28*, 1761–1775.
- [11] M. H. Petersen, O. Hagemann, K. T. Nielsen, M. Jørgensen, F. C. Krebs, *Sol. Energy Mater. Sol. Cells.* **2007**, *91*, 996–1009.
- [12] E. Bundgaard, F. C. Krebs, *Sol. Energy Mater. Sol. Cells.* **2007**, *91*, 1019–1025.
- [13] B. C. Thompson, Y. G. Kim, J. R. Reynolds, *Macromolecules.* **2005**, *38*, 5359–5362.
- [14] B. C. Thompson, Y. G. Kim, T. D. McCarley, J. R. Reynolds, *J. Am. Chem. Soc.* **2006**, *128*, 12714–12725.
- [15] L. M. Andersson, Z. Fengling, I. Olle, *Appl. Phys. Lett.* **2007**, *91*, 071108–3.
- [16] L. H. Slooff, S. C. Veenstra, J. M. Kroon, D. J. D. Moet, J. Sweelssen, M. M. Koetse, *Appl. Phys. Lett.* **2007**, *90*, 143506–3.

- [17] D. Mühlbacher, M. Scharber, M. Morana, Z. Zhu, D. Waller, R. Gaudiana, C. Brabec, *Adv. Mater.* **2006**, *18*, 2884–2889.
- [18] J. Peet, J. Y. Kim, N. E. Coates, W. L. Ma, D. Moses, A. J. Heeger, G. C. Bazan, *Nat. Mater.* **2007**, *6*, 497–500.
- [19] M. Zhang, H. N. Tsao, W. Pisula, C. Yang, A. K. Mishra, K. Müllen, *J. Am. Chem. Soc.* **2007**, *129*, 3472–3473.
- [20] M. Leclerc, *J. Polym. Sci. Part A* **2001**, *39*, 2867–2873.
- [21] L. Akcelrud, *Prog. Polym. Sci.* **2003**, *28*, 875–962.
- [22] J. F. Morin, M. Leclerc, D. Adès, A. Siove, *Macromol. Rapid Commun.* **2005**, *26*, 761–778.
- [23] J. V. Grazulevicius, P. Strohriegel, J. Pielichowski, K. Pielichowski, *Prog. Polym. Sci.* **2003**, *28*, 1297–1353.
- [24] N. Drolet, J. F. Morin, N. Leclerc, S. Wakim, Y. Tao, M. Leclerc, *Adv. Funct. Mater.* **2005**, *15*, 1671–1682.
- [25] J. Li, F. Dierschke, J. Wu, A. C. Grimsdale, K. Müllen, *J. Mater. Chem.* **2006**, *16*, 96–100.
- [26] N. Blouin, A. Michaud, M. Leclerc, *Adv. Mater.* **2007**, *19*, 2295–2300.
- [27] L. J. A. Koster, V. D. Mihailetschi, *Appl. Phys. Lett.* **2006**, *88*, 093511–3.
- [28] D. M. de Leeuw, M. M. J. Simenon, A. R. Brown, R. E. F. Einerhand, *Synth. Met.* **1997**, *87*, 53–59.
- [29] S. A. Choulis, J. Nelson, Y. Kim, D. Poplavskyy, T. Kreouzis, J. R. Durrant, D. D. C. Bradley, *Appl. Phys. Lett.* **2003**, *83*, 3812–3814.
- [30] V. D. Mihailetschi, J. K. J. Van Duren, P. W. M. Blom, J. C. Hummelen, R. A. J. Janssen, J. M. Kroon, M. T. Rispens, W. J. H. Verhees, M. M. Wienk, *Adv. Funct. Mater.* **2003**, *13*, 43–46.
- [31] S. H. Park, A. Roy, S. Beaupré, S. Cho, N. Coates, J. S. Moon, D. Moses, M. Leclerc, K. Lee, A. J. Heeger, *Nat. Photonics* **2009**, *3*, 297–302.
- [32] Y. Li, Q. Guo, Z. Li, J. Pei, W. Tian, *Energy Environ. Sci.* **2010**, *3*, 1427–1436.
- [33] S. D. Collins, N. A. Ran, M. C. Heiber, T. Q. Nguyen, *Adv. Energy Mater.* **2017**, *7*, 1602242–8.
- [34] S. A. H. Vuai, N. S. Babu, *Des. Monomers Polym.* **2021**, *24*, 123–135.
- [35] N. S. Babu, S. A. H. Vuai, *Des. Monomers Polym.* **2021**, *24*, 224–237.
- [36] T. Mohr, V. Aroulmoji, R. Samson Ravindran, M. Müller, S. Ranjitha, G. Rajarajan, P. M. Anbarasan, *Spectrochim. Acta Part A* **2015**, *135*, 1066–1073.
- [37] X. H. Xie, W. Shen, R. X. He, M. Li, *Bull. Korean Chem. Soc.* **2013**, *34*, 2995–3004.
- [38] A. D. Becke, *J. Chem. Phys.* **1993**, *98*, 5648–5652.
- [39] Gaussian 09, Revision C.01, M. J. Frisch, G. W. Trucks, H. B. Schlegel, G. E. Scuseria, M. A. Robb, J. R. Cheeseman, G. Scalmani, V. Barone, G. A. Petersson, H. Nakatsuji, X. Li, M. Caricato, A. Marenich, J. Bloino, B. G. Janesko, R. Gomperts, B. Mennucci, H. P. Hratchian, J. V. Ortiz, A. F. Izmaylov, J. L. Sonnenberg, D. Williams-Young, F. Ding, F. Lipparini, F. Egidi, J. Goings, B. Peng, A. Petrone, T. Henderson, D. Ranasinghe, V. G. Zakrzewski, J. Gao, N. Rega, G. Zheng, W. Liang, M. Hada, M. Ehara, K. Toyota, R. Fukuda, J. Hasegawa, M. Ishida, T. Nakajima, Y. Honda, O. Kitao, H. Nakai, T. Vreven, K. Throssell, J. A. Montgomery, Jr., J. E. Peralta, F. Ogliaro, M. Bearpark, J. J. Heyd, E. Brothers, K. N. Kudin, V. N. Staroverov, T. Keith, R. Kobayashi, J. Normand, K. Raghavachari, A. Rendell, J. C. Burant, S. S. Iyengar, J. Tomasi, M. Cossi, J. M. Millam, M. Klene, C. Adamo, R. Cammi, J. W. Ochterski, R. L. Martin, K. Morokuma, O. Farkas, J. B. Foresman, D. J. Fox, Gaussian, Inc., Wallingford CT, **2009**.
- [40] G. Parr, W. Yang, *Density-Functional Theory of Atoms and Molecules*. New York University Press, Oxford, **1989**.
- [41] J. Tomasi, B. Mennucci, R. Cammi, *Chem. Rev.* **2005**, *105*, 2999–3093.
- [42] N. M. O’Boyle, A. L. Tenderholt, K. M. Langner, *J. Comb. Chem.* **2008**, *29*, 839–845.
- [43] S. E. Shaheen, C. J. Brabec, N. S. Sariciftci, F. Padinger, T. Fromherz, J. C. Hummelen, *Appl. Phys. Lett.* **2001**, *78*, 841–843.
- [44] Z. Wu, B. Fan, F. Xue, C. Adachi, J. Ouyang, *Sol. Energy Mater. Sol. Cells.* **2010**, *94*, 2230–2237.
- [45] M. C. Scharber, D. Mühlbacher, M. Koppe, P. Denk, C. Waldauf, A. J. Heeger, C. J. Brabec, *Adv. Mater.* **2006**, *18*, 789–794.
- [46] C. J. Brabec, A. Cravino, D. Meissner, N. S. Sariciftci, T. Fromherz, M. T. Rispens, L. Sanchez, J. C. Hummelen, L. Sanchez, *Adv. Funct. Mater.* **2001**, *11*, 374–380.
- [47] H. Frohne, S. E. Shaheen, C. J. Brabec, D. C. Müller, N. S. Sariciftci, K. Meerholz, *ChemPhysChem* **2002**, *3*, 795–799.
- [48] L. J. A. Koster, V. D. Mihailetschi, P. W. M. Blom, *Appl. Phys. Lett.* **2006**, *88*, 052104–8.
- [49] B. Minnaert, M. Burgelman, *Prog. Photovolt. Res. Appl.* **2007**, *15*, 741–748.
- [50] R. G. Pearson, *Proc. Natl. Acad. Sci. USA* **1986**, *83*, 8440–8441.

Manuscript received: November 24, 2021

Revised manuscript received: December 27, 2021